






## Measurement and Performance Evaluation of an IoT-Integrated Dehumidification Control System for Airborne Infection Isolation Rooms: A Case Study at Betong Hospital

Thawin Matung<sup>1</sup>, Prasit Nangtin<sup>1\*</sup>, Thammanoon Sookchaiya<sup>2</sup>

<sup>1</sup> Department of Electrical Engineering, Pathumwan Institute of Technology Bangkok 10330, Thailand

<sup>2</sup> Department of Electrical Power, Samutsakorn Technical College, Samutsakhon 74000, Thailand

Corresponding Author Email: [prasit@pit.ac.th](mailto:prasit@pit.ac.th)

Copyright: ©2025 The authors. This article is published by IETA and is licensed under the CC BY 4.0 license (<http://creativecommons.org/licenses/by/4.0/>).

<https://doi.org/10.18280/i2m.240303>

### ABSTRACT

**Received:** 29 April 2025

**Revised:** 30 May 2025

**Accepted:** 11 June 2025

**Available online:** 30 June 2025

#### Keywords:

*airborne infectious isolation rooms, humidity control, desiccant dehumidification system, Internet of Things, real-time monitoring*

This study presents the measurement, and performance evaluation of an IoT-integrated humidity control system for airborne infection isolation rooms (AIIRs), developed in accordance with ASHRAE Standard 170. The system features two silica gel panels that operate alternately between dehumidification and regeneration, allowing continuous and efficient humidity regulation. Environmental monitoring is carried out using a BME280 sensor and an ESP32 microcontroller, providing real-time measurements of temperature and relative humidity. Data are transmitted to Google Firebase and Sheets for cloud-based storage, analysis, and visualization, and are used to assess system performance. A notification system with a front display and smartphone application alerts users when environmental conditions exceed acceptable thresholds. Experimental results show that the system maintained an average temperature of 22.63°C and relative humidity at 54.37% RH, both within recommended limits for infection control. The humidity ratio was 0.00882 kg/kg·da, below the ASHRAE threshold of 0.012 kg/kg·da. Each silica gel panel sustained RH below 60% for approximately 1.3 hours and was fully regenerated at 100°C within 55 minutes. Overall, the system demonstrates reliable, real-time environmental control and offers a cost-effective solution for enhancing indoor air quality and strengthening safety for both patients and healthcare personnel in airborne infection isolation rooms.

## 1. INTRODUCTION

Airborne transmission of infectious agents in healthcare settings is a critical issue in global medicine and public health. tuberculosis, an airborne-transmissible disease, poses a significant challenge due to its increasing incidence and the emergence of multidrug-resistant tuberculosis (MDR-TB). Moreover, respiratory infectious diseases caused by emerging pathogens, such as SARS, avian influenza (A H5N1), and COVID-19, have demonstrated the potential for airborne or aerosol transmission under certain conditions [1-5].

Airborne infectious diseases remain a significant public health concern, particularly in enclosed environments. COVID-19 alone has resulted in over 472 million confirmed cases and 6 million deaths globally since late 2019 [1]. The virus's capacity to transmit via fine aerosols (<5 µm) necessitates robust environmental controls, especially in high-risk settings such as airborne infection isolation rooms (AIIRs) [6, 7]. Environmental conditions also affect transmission rates; for instance, a study by Wu et al. [8]. Pöhlker et al. [9] reviewed the dynamics of respiratory droplets and aerosols, emphasizing their key role in transmitting airborne pathogens such as tuberculosis, influenza, and SARS-CoV-2. They noted that fine aerosols (<5 µm) can remain airborne for long periods and travel considerable distances, increasing infection risk in

enclosed spaces. The study highlights the need for integrated environmental controls such as ventilation, air filtration, and humidity regulation to reduce airborne transmission, especially in high-risk areas like AIIRs. Preventing airborne transmission of infectious agents in healthcare facilities requires effective and well-implemented measures. Air quality control can be achieved through various environmental management strategies to reduce the risk of airborne infections [10]. These include introducing fresh outdoor air, maintaining pressure differentials between areas, controlling airflow direction, utilizing air filtration systems, employing ultraviolet (UV) lamps, and regulating temperature and relative humidity levels. Each air quality control strategy plays a distinct role in mitigating airborne infection risks, particularly in AIIRs. Ventilation with outdoor air promotes dilution of airborne contaminants by increasing the air change rate per hour (ACH); at least 2 ACH of outdoor air and a total of 12 ACH are recommended to ensure adequate dilution [11]. Pressure differential control supports containment by maintaining negative pressure between the isolation room and adjacent areas, directing airflow inward and preventing contaminated air from escaping [12, 13]. High-efficiency air filtration, especially using HEPA filters, removes ≥99.97% of airborne particles ≥0.3 µm, including Mycobacterium tuberculosis and SARS-CoV-2, thereby reducing aerosol recirculation [14, 15].

The integrated application of these three strategies ventilation, pressure control, and filtration provides a multilayered defense against airborne transmission, particularly in tropical settings where high humidity and temperature can enhance pathogen viability [16]. According to the Centers for Disease Control and Prevention (CDC) and the American Society of Heating, Refrigerating and Air-Conditioning Engineers (ASHRAE), significant emphasis has been placed on the Heating, Ventilation, and Air Conditioning (HVAC) in hospitals. These organizations have established standards and guidelines to mitigate the spread of diseases such as COVID-19, MERS, SARS, and tuberculosis within hospitals and residential buildings. Temperature and relative humidity (RH) are key environmental factors that influence the survival and transmission of airborne pathogens. Lower temperatures ( $<20^{\circ}\text{C}$ ) enhance the structural stability of viral lipid membranes and protein capsids, prolonging viability especially for respiratory viruses such as influenza and SARS-CoV-2 [17, 18]. RH affects both droplet behavior and pathogen stability. At low RH ( $<40\%$ ), respiratory droplets evaporate quickly, forming droplet nuclei ( $\leq 5\text{ }\mu\text{m}$ ) that remain airborne for extended periods, enabling long-range transmission [19]. High RH ( $>80\%$ ), in contrast, maintains droplet size and promotes rapid settling, which reduces airborne persistence but may increase surface contamination [20]. Pathogen sensitivity to RH varies: while influenza virus is more stable at low RH, others like respiratory syncytial virus (RSV) and some coronaviruses persist better at intermediate RH ( $\sim 50\%$ ). Mechanistically, humidity influences salt concentration and pH within evaporating droplets, which affects capsid integrity and viral infectivity. Combined effects of RH and temperature also shape aerosol dispersion, stratification, and ventilation efficiency in enclosed environments, significantly impacting infection risk in settings such as AIIRs [21, 22]. Controlling temperature and relative humidity helps to reduce the spread and growth of airborne pathogens, as illustrated in Figure 1 [23].

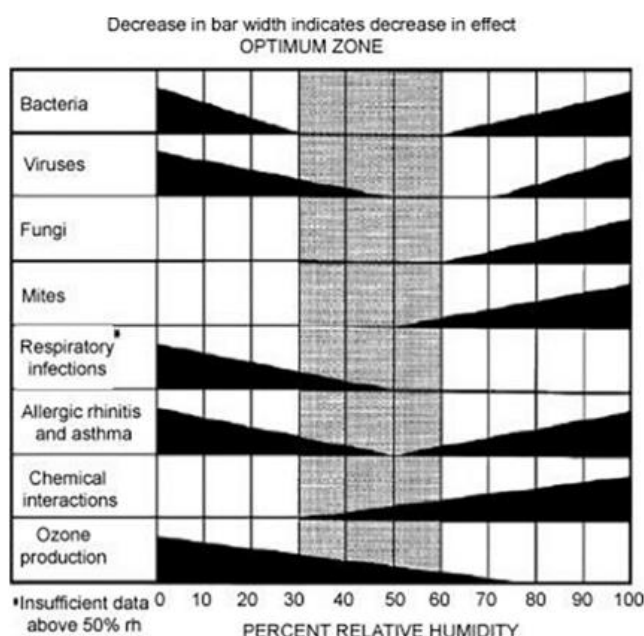


**Figure 1.** Influence of relative humidity on the respiratory system and the survival of pathogens [23]

Maintaining indoor air temperature and relative humidity in healthcare facilities, especially in negative-pressure AIIRs is

essential. Still, it remains a challenge due to the hot and humid climate in Thailand. Conventional air conditioning systems often fail to regulate humidity effectively. According to ASHRAE STD 170 and CDC guidelines, AIIRs must maintain a temperature between  $21\text{--}24^{\circ}\text{C}$  and a relative humidity level between  $40\text{--}60\%$  RH, with a minimum of 12 air changes per hour. However, continuous air exhaust and the high humidity of incoming fresh air make it difficult to achieve these conditions [24, 25].

A case study of Betong Hospital, located in Betong district, Yala province, Thailand a highland area surrounded by mountains with a hot and humid climate and consistently high relative humidity throughout the year is illustrated in Figure 2.

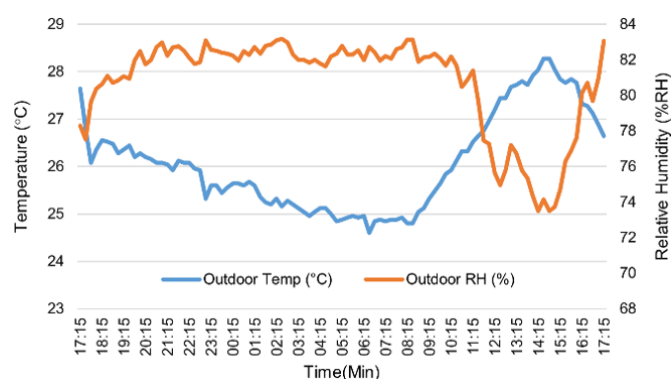


**Figure 2.** Outdoor air temperature and relative humidity at Beong Hospital

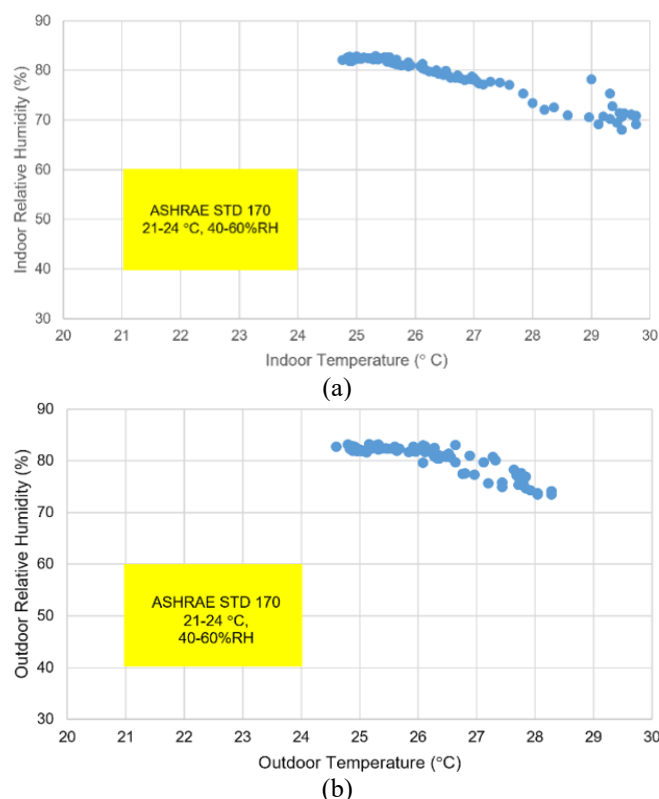


**Figure 3.** Distribution of temperature and relative humidity indoor and outdoor AIIRs

Figures 3 (a)-(b) show the results of the analysis of temperature and relative humidity values indoor and outdoor the AIIRs with the ASHRAE STD 170 standards. The yellow band represents the acceptable range according to the standards, which is  $21\text{--}24^{\circ}\text{C}$  for temperature and  $40\text{--}60\%$  RH

for relative humidity. The blue clusters indicate the measured temperature and relative humidity values indoor and outdoor the AIIRs. These values fall outside the acceptable range specified by the standards.

Under environmental conditions where temperature and relative humidity exceed safety thresholds, researchers developed an environmental control system for negative-pressure airborne infection isolation rooms. The system regulates temperature and relative humidity using alternating silica gel panels for dehumidification and regeneration. Real-time monitoring ensures continuous environmental assessment. The objective of this study is to evaluate the performance of an IoT-integrated dehumidification control system and its ability to maintain safe environmental conditions. It also seeks to understand how effectively the system controls humidity and temperature, and which indicators best reflect its operational reliability in a clinical context. The system effectively reduces airborne infection risks from bacteria, viruses, fungi, and dust mites, enhancing safety for patients and healthcare personnel. It is especially vital during infectious disease outbreaks to support controlled environments and reinforce confidence in patient care.

## 2. LITERATURE REVIEW

Hamdani et al. [26] studied an HVAC control system for a negative pressure isolation room at Syiah Kuala University Hospital. The system was designed to maintain negative air pressure and stable airflow to meet infection control standards. Results showed that the system effectively maintained safe environmental conditions, supporting its role in airborne infection prevention.

Similarly, the work by Mehare et al. [27] evaluated a rotary dehumidifier with molecular sieve desiccants operating under coupled regeneration mode. This approach optimized moisture removal and energy efficiency by leveraging waste heat recovery, highlighting desiccant-based systems' potential in sustainable humidity control.

Wang et al. [28] emphasized the need for optimizing airflow direction and diffuser placement in AIIRs to enhance negative pressure stability and infection control. Their research supports the necessity for precision in HVAC component configuration.

In addition, Nie et al. [29] compared novel solid desiccants with conventional materials, finding that MIL-101(Cr) showed up to six times higher moisture adsorption than silica gel, thereby promoting enhanced dehumidification in hospital settings. Such findings are critical for improving adsorbent selection in AIIRs.

Urrutia et al. [30] evaluated advanced air purification technologies across multiple healthcare environments. Their findings demonstrated significant clinical and environmental benefits, particularly in reducing airborne contaminants. This supports the integration of air purification as a complementary measure to conventional HVAC systems.

Stevenson et al. [31] proposed a paradigm shift in infection control, emphasizing airborne transmission as a key route for disease spread. Their study reinforced the need for environmental systems that prioritize humidity and airflow control to reduce pathogen survivability and transmission in indoor spaces.

Building on this, Thornton et al. [32] conducted a systematic review focusing on HVAC design features,

particularly the impact of humidity on viral transmission. The study concluded that maintaining relative humidity within an optimal range could significantly reduce the viability and dispersion of respiratory viruses, including SARS-CoV-2.

From a control engineering perspective, Bahramnia et al. [33] applied model predictive control (MPC) to HVAC systems for precise regulation of temperature and humidity. Their results highlighted that advanced control algorithms can enhance indoor air quality by dynamically adjusting environmental parameters based on real-time feedback, making such approaches suitable for critical environments like airborne infection isolation rooms.

Thiyaneswaran et al. [34] developed an IoT-based temperature monitoring and alert system for vaccination containers that integrates sensors and microcontrollers to track temperature variations. Their system triggers real-time alerts using buzzer and lamp modules when temperature exceeds defined thresholds, enhancing rapid response capabilities in cold chain applications.

Similarly, Ali and Khan [35] proposed a multi-methods decision-making model to assess IoT platforms for COVID-19 vaccine transportation. The study highlighted the importance of selecting appropriate platforms based on functionality, flexibility, and alert capabilities to ensure effective tracking and risk management throughout the cold chain process.

Jiang et al. [36] introduced a sustainable cold chain management framework based on IoT, focusing on the integration of real-time sensors and cloud-based data storage using Firebase. The framework demonstrated how centralized monitoring and alerting could maintain consistent environmental conditions, contributing to the overall resilience of vaccine distribution systems.

Hassan et al. [37] developed an IoT-based health monitoring system that tracks temperature, blood pressure, and sleep patterns to support chronic disease management. By integrating multiple sensors with cloud-based platforms, their system enables real-time data collection, alerts, and remote access for healthcare providers. The study emphasizes the potential of IoT to reduce hospital visits and improve patient outcomes, while also noting challenges such as data security and energy efficiency.

Ghani et al. [38] proposed an AI-based scheduling system designed to support rehabilitation and home health monitoring for patients with coronary artery disease and other cardiovascular conditions. The system integrates IoT data with artificial intelligence to optimize monitoring schedules and personalize care. Their findings show that AI-enhanced IoT applications can improve treatment adherence, reduce hospital readmissions, and support long-term health management from home.

Rahita et al. [39] reviewed ten years of research on the application of IoT in structural health monitoring. Their analysis highlights how IoT technologies have transformed monitoring practices through real-time data acquisition, remote diagnostics, and predictive maintenance. Although the study focuses on infrastructure, its insights underscore the adaptability of IoT systems to various domains including healthcare by demonstrating the scalability, sensor integration, and data-driven decision-making that IoT enables.

AbdelRaheem et al. [40] presented the design and deployment of a synchronized IoT-based structural health monitoring system. Their framework demonstrates the capability of IoT to provide real-time, coordinated data from multiple sensors for enhanced structural analysis. While

centered on infrastructure, the study reinforces the broader utility of IoT systems in precision monitoring, timely alerts, and system integration principles that are equally valuable in healthcare and other critical applications.

Nasution et al. [41] demonstrated that a webcam-based contactless respiratory rate monitoring system achieved high accuracy and repeatability, particularly when imaging the collarbone area. Their findings highlight the potential of low-cost imaging systems for continuous vital sign monitoring in clinical environments.

### 3. METHODS

The study on the operation of airborne infectious isolation rooms referenced the ANSI/ASHRAE/ASHE Standard 170-2017: Ventilation of Health Care Facilities and data from the U.S. Centers for Disease Control and Prevention (CDC). It also included field data collection at Betong Hospital in Betong district, Yala province. Based on this information, the researcher applied these findings to the design and development of airborne infectious isolation rooms at the Department of electrical technology, Yala technical college, Mueang District, Yala province, following the guidelines established by the Engineering Institute of Thailand [42].

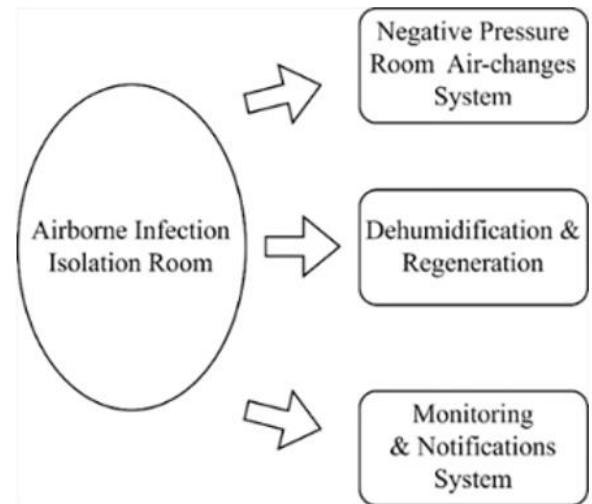
Figure 4 illustrates the components of an airborne infectious isolation rooms designed to control the environmental conditions in the room to prevent the spread of airborne pathogens to the external environment. The design and development of this system concentrate on key aspects, such as the design of the relative humidity control system, the assessment of humidity dehumidification efficiency, and the creation of a monitoring and notifications system.

Table 1 specifies that air pressure must not exceed -2.5 Pascals to maintain negative pressure within the room. The recommended temperature range is 21–24°C, with relative humidity between 40–60%. Additionally, an air change rate of at least 12 ACH is required to ensure consistent air exchange

within airborne infection isolation rooms.

**Table 1.** Parameters that must be maintained within standard limits

No.	Parameter	Value
1	Air Pressure	< -2.5 Pa
2	Air Temperature	21-24°C
3	Relative Humidity	40 – 60% RH
4	Air Change Rates	>12 ACH



**Figure 4.** Components of the airborne infectious isolation rooms control system

#### 3.1 AIIRs

In this study, researchers constructed an airborne infection isolation room with negative pressure in accordance with the Model 3 standards of the Engineering Institute of Thailand. Figure 5 presents the AIIRs design, while Figure 6 provides an image of the actual room.

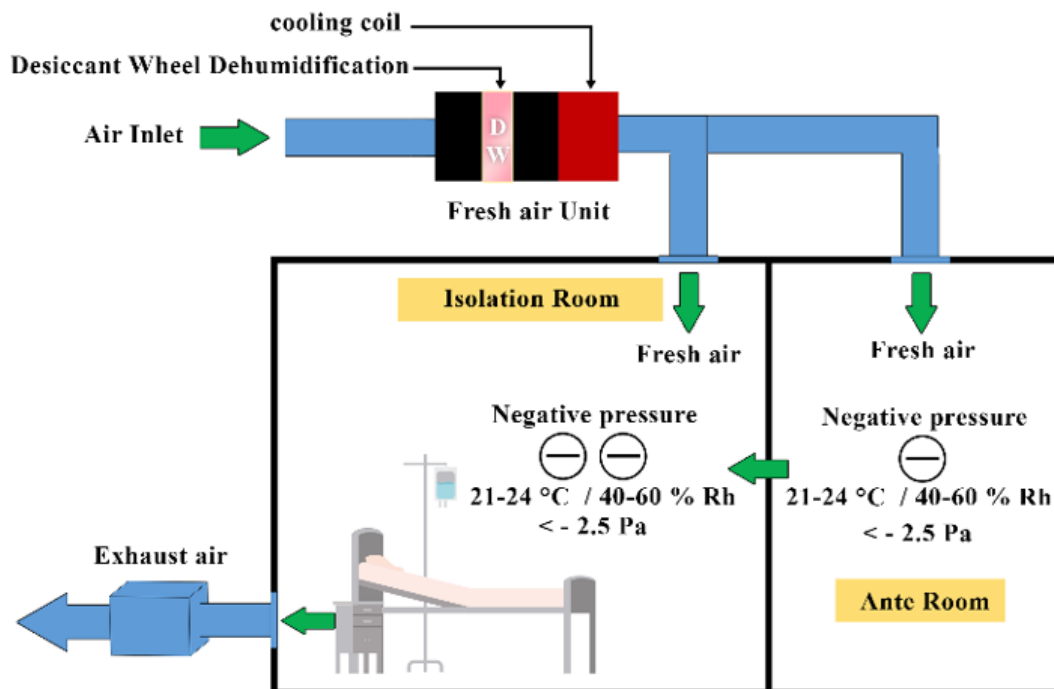


**Figure 5.** AIIRs specifications



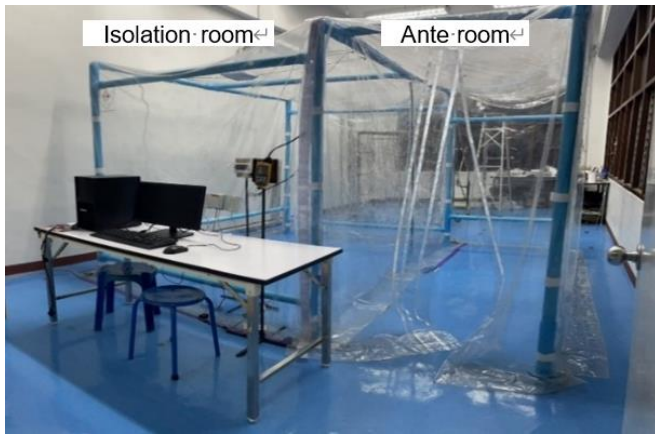


**Figure 6.** AIIRs based on model 3 of the EIT

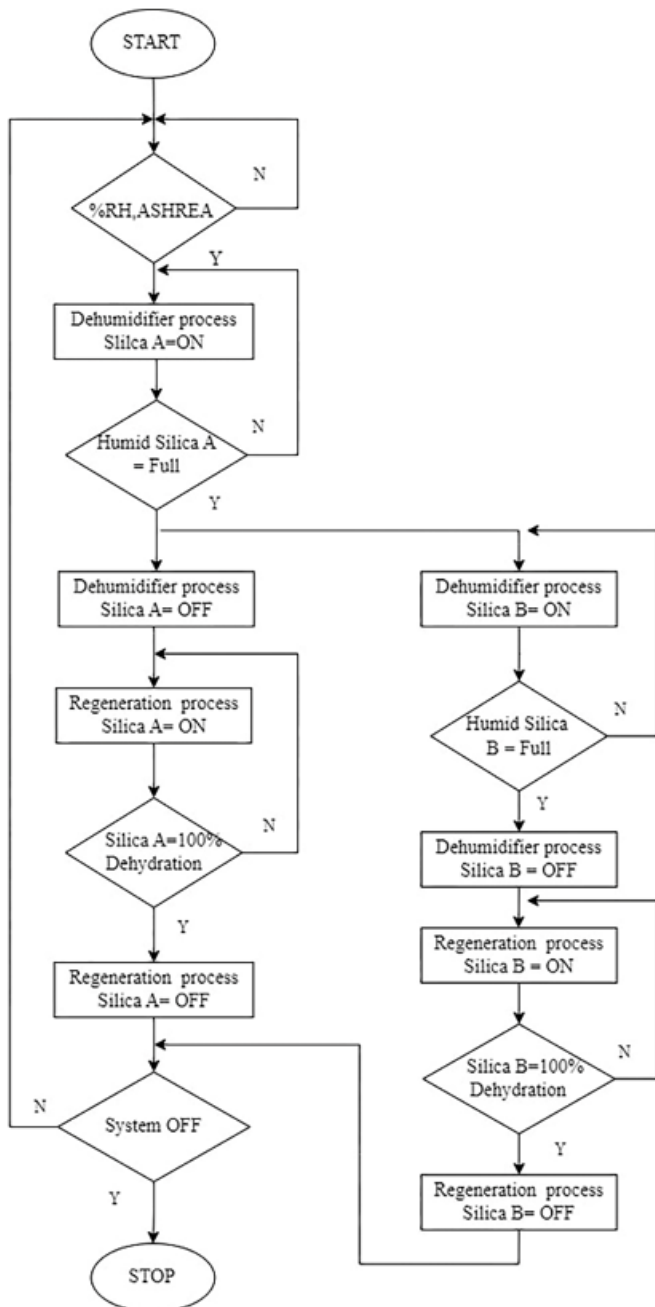


**Figure 7.** Flowchart of silica gel dehumidification and regeneration process

### 3.2 Control system for dehumidification and regeneration

The environmental control system developed in this study employs alternating silica gel panels that function in a cyclical process of dehumidification and regeneration. During each cycle, one panel adsorbs moisture from incoming air while the other undergoes regeneration through the application of heat, typically via warm air, to restore its moisture absorption capacity. This configuration enables continuous humidity control without interrupting airflow or inducing thermal instability [43]. Unlike conventional air conditioning (AC) systems, which achieve dehumidification as a secondary effect by cooling air below its dew point through energy-intensive refrigeration cycles, the silica gel system directly targets moisture removal [44]. As a result, it delivers higher energy efficiency and better environmental stability, particularly in AIIRs, where precise humidity control is essential for infection prevention and patient well-being [45]. The system's modular design further enhances operational flexibility and adaptability under varying environmental conditions [46].

The dehumidification and regeneration process using silica gel in an environmental control system the dehumidification and regeneration process in an environmental control system is designed to ensure efficient humidity control by alternating between two silica gel units, Silica A and Silica B.

Figure 7 illustrates the operation of a dual-unit silica gel system designed for continuous humidity control. Initially, the system measures relative humidity and compares it to predefined standards. If the humidity exceeds the threshold, Silica A is activated to absorb moisture until saturation. Once saturation is reached, Silica A enters the regeneration phase, and the system switches to activate Silica B for moisture absorption. This alternating process allows one unit to regenerate while the other dehumidifies, ensuring uninterrupted operation. The cycle repeats until humidity levels stabilize within the target range, enhancing environmental control efficiency, particularly in critical settings such as isolation rooms.

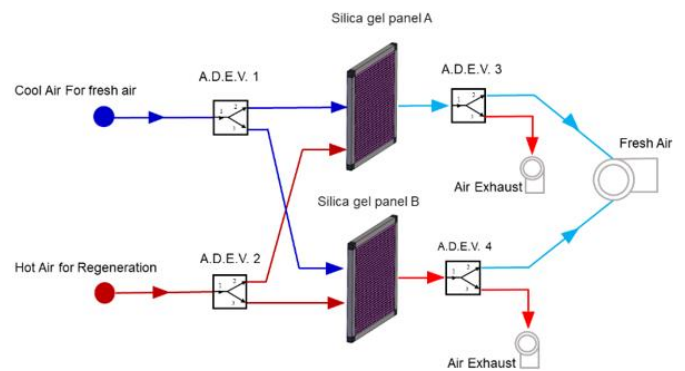


**Figure 8.** Dehumidification system using silica gel desiccant

A.D.E.V = Air Damper Electric Valve

**State 1:**

A.D.E.V. 1: ON = position 1-2, OFF, position 3 A.D.E.V. 3: ON, position 1-2, OFF, position 3

A.D.E.V. 2: ON= position 1-3, OFF, position 2 A.D.E.V. 4: ON, position 1-3, OFF, position 2

**State 2:**

A.D.E.V. 1: ON = position 1-3, OFF, position 2 A.D.E.V. 3: ON, position 1-3, OFF, position 2

A.D.E.V. 2: ON= position 1-3, OFF, position 2 A.D.E.V. 4: ON, position 1-3, OFF, position 2

A.D.E.V. 2: ON= position 1-2, OFF, position 3 A.D.E.V. 4: ON, position 1-2, OFF, position 3

Figure 8 illustrates the overall process of dehumidification and regeneration using a dual-panel silica gel system. Air damper electric valves (A.D.E.V.) are used to regulate airflow throughout the system. Specifically, A.D.E.V. 1 and A.D.E.V. 2 control the air intake into silica gel panels A and B, respectively, while A.D.E.V. 3 and A.D.E.V. 4 manage air discharge with two distinct roles. A.D.E.V. 3 directs hot exhaust air from the regeneration process out of the system to prevent heat accumulation, whereas A.D.E.V. 4 delivers conditioned fresh air from the dehumidification process into the isolation room. The functions of these valves alternate based on the operating cycle. In the dehumidification mode, incoming cold air typically below 12°C with relative humidity above 80% RH is passed through a silica gel panel. As the air flows through, moisture is absorbed by the silica gel, reducing the relative humidity to below 60% RH. During this process, the silica gel gradually changes color from blue to pink, indicating that it has reached saturation. Once fully saturated, the silica gel undergoes a regeneration phase in which hot air, approximately 100°C, is passed through the panel to desorb the absorbed moisture. The silica gel then returns to its original blue color, indicating readiness for the next dehumidification cycle. The system is designed to alternate between dehumidification and regeneration every 1 hour and 30 minutes. While one silica gel panel is regenerating, the other actively dehumidifies the air, enabling continuous operation without interruption. In this experiment, 2 kg of silica gel was used, with an air suction velocity of 8.76 m/s and an airflow rate of 156 CFM, demonstrating effective and reliable humidity control suitable for AIIRs.

The environmental control system in AIIRs includes a fresh air inlet, ante room, and negative-pressure isolation room. Filtered air enters to maintain air balance, while the ante room adds a barrier against contamination. The isolation room uses silica gel panels for humidity control and negative pressure to contain airborne pathogens. An electric air damper regulates airflow to enhance infection control, as shown in Figure 9.

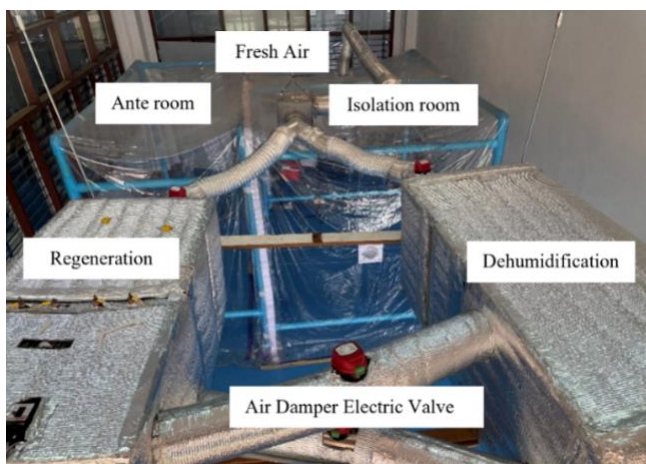


**Figure 9.** Silica gel desiccant-based dehumidification system components

### 3.3 Measuring instruments

Various physical parameters within AIIRs operating under negative pressure were systematically measured in this study.

Temperature and relative humidity were recorded using the SL300TH Data Logger, while air velocity was assessed via the FLUKE 922 Digital Anemometer. To capture high-temperature conditions during the regeneration process, a YUGO MY-64 multimeter in conjunction with a Type K thermocouple was employed. Detailed specifications of the measuring instruments utilized are presented in Table 2.

**Table 2.** Specifications of measuring instruments

Equipment	Measuring Property	Range	Accuracy
Supco SL300 TH	Temperature Relative Humidity Range	-40°C to 158°C RH 0 to 99%	+/- 0.5°C, +/-2% RH
YUGO Series MY-64 with Thermocouple Type K	Temperature	-20°C-1000°C	+/-1%
FLUKE 922 Digital Anemometer	Air Velocity	250-16,000 fpm 1-80 m/s	+/-2.5%

### 3.4 Measurement data analysis

The mathematical modeling of dehumidification performance and Moisture Removal Capacity is described in this section [47, 48].

$$\eta_{deh} = \frac{\omega_1 - \omega_2}{\omega_1} \quad (1)$$

$$\omega = 0.62198 \frac{p_w}{(p - p_w)} \quad (2)$$

The Moisture Removal Capacity (MRC) represents the mass flow rate of moisture removed.

$$MRC = \rho V_{deh} (\omega_1 - \omega_2) \quad (3)$$

### 3.5 Monitoring and notifications system

The monitoring and notification system installed at the entrance of airborne infectious isolation rooms (AIIRs) is designed to monitor essential environmental conditions, particularly temperature and humidity.

The system collects and processes the data locally before transmitting it to a cloud-based platform, allowing for real-time access and data recording. Current readings are clearly displayed on a screen outside the isolation room, enabling healthcare staff to quickly assess conditions without entering the room. If any value falls outside the defined safety range, the system automatically triggers visual and audio alerts to inform staff of the abnormality. The structure and function of the system are illustrated in Figure 10 which presents the block diagram of its operation.

Figure 11 shows details of the monitoring and alert system for airborne infectious isolation rooms (AIIRs). A BME280 sensor measures temperature and humidity, sending data via a Node MCU (ESP32) to Google Firebase for real-time monitoring and Google Sheets for record-keeping. If values exceed safety thresholds, another Node MCU activates a

buzzer and warning light at the room entrance. Users can check real-time data via smartphone, allowing quick responses to abnormal conditions. The system ensures continuous environmental control and enhances safety for patients and staff.

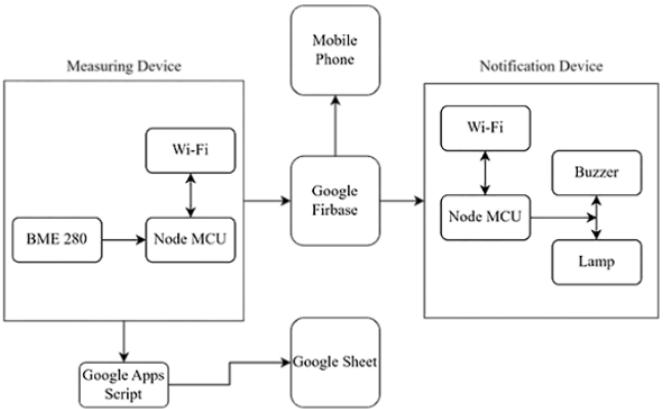


**Figure 10.** Block diagram of the monitoring and notifications system

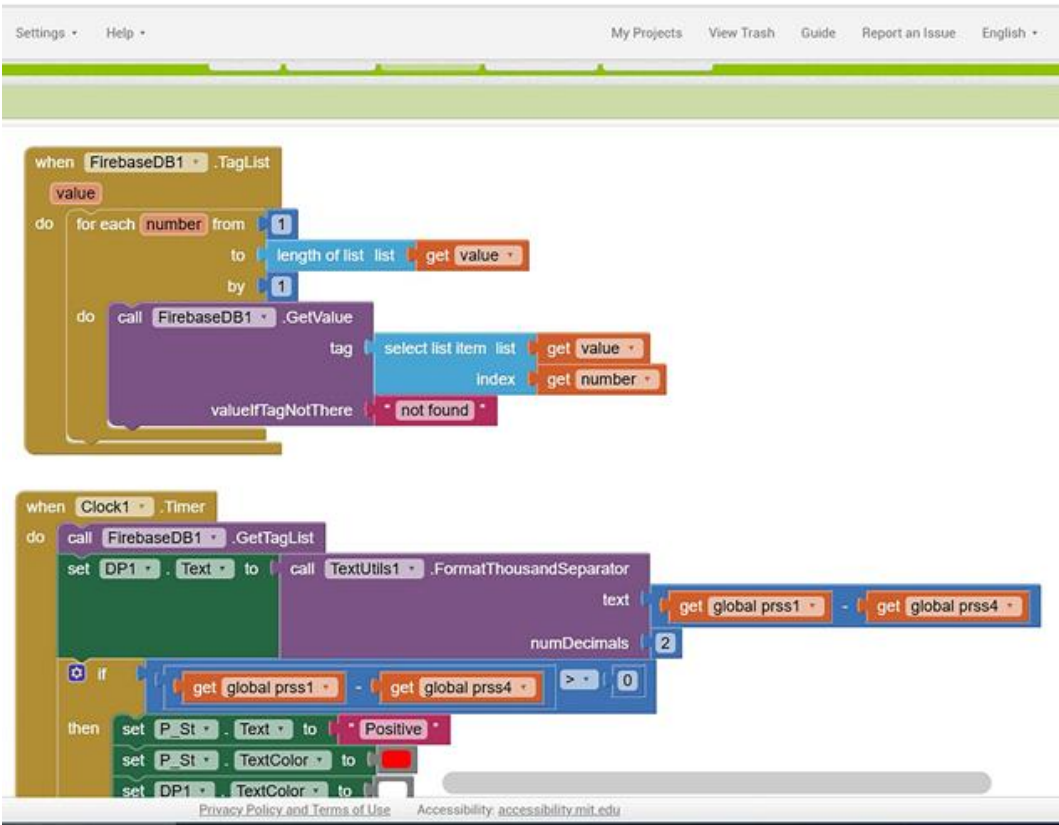
Figure 12 illustrates the programming process for the IoT control system using MIT App Inventor, a visual programming tool for developing mobile applications. The image displays the block-based commands used to connect and control environmental monitoring components, such as receiving data from the BME280 sensor via Node MCU and displaying the measured values in a user-friendly format on a smartphone interface.

Figure 13 shows the script written in Google Apps Script, which is used to manage data transmitted from Firebase to Google Sheets in a cloud-based system. This script handles

data integration from sensing devices, including timestamp logging, temperature, and relative humidity values. It also provides automatic notifications when measured parameters exceed the defined thresholds. This enables system operators to monitor the status of airborne infection isolation rooms in real time without being physically present.



**Figure 11.** Details of the monitoring and notifications system



**Figure 12.** Programming with MIT App Inventor for IoT system control



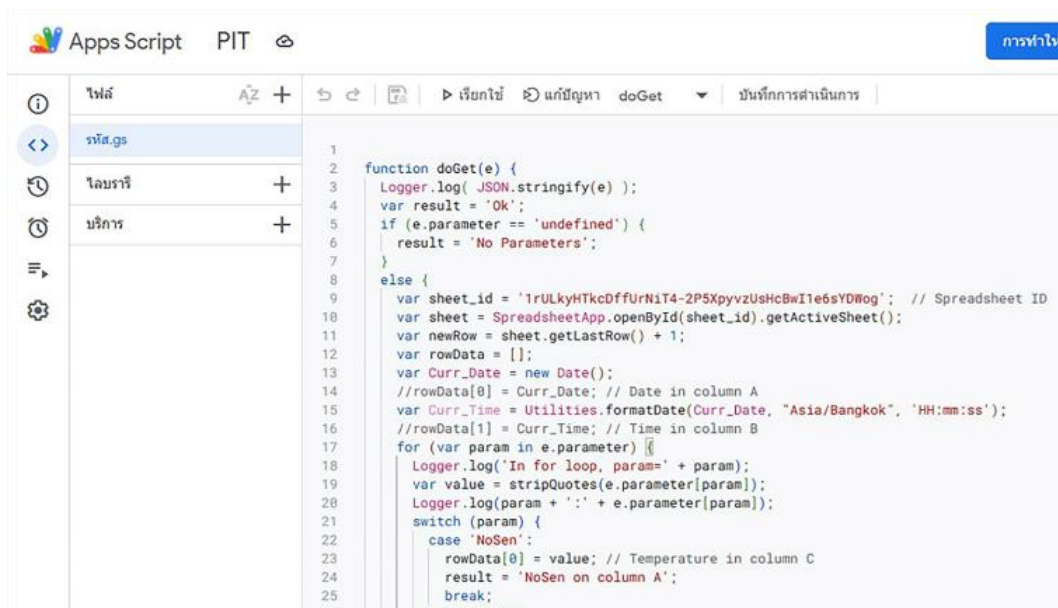


Figure 13. Google Apps Script

## 4. RESULTS AND DISCUSSIONS

A temperature and humidity control system was developed for airborne infection isolation rooms to maintain conditions within 21–24°C and 40–60% RH, in accordance with ASHRAE Standard 55/170-2017 and ISO 7730. The experiment, conducted under real weather conditions similar to Betong Hospital, ensures accuracy and reliability.

### 4.1 Dehumidification process for AIIRs

This study presents the development and evaluation of a system for precise measurement and control of temperature and relative humidity in airborne infection isolation rooms, with a focus on the dehumidification process to ensure that indoor environmental conditions comply with recommended standards. The dehumidification system consists of two identical panels, designated as Silica Gel A and Silica Gel B, to differentiate their alternating roles in the adsorption regeneration cycle. Each panel measures 30 cm × 30 cm and is filled with approximately 2 kilograms of spherical silica gel

beads. The silica gel exhibits an average pore diameter of 2.5 nanometers, a specific surface area of around 750 m<sup>2</sup>/g, and an equilibrium adsorption capacity of up to 37% of its dry weight at 100% relative humidity. These properties enable efficient moisture removal from the air in a negative-pressure isolation room environment. By operating in alternating cycles where one panel adsorbs moisture and the other undergoes thermal regeneration using heated air the system maintains continuous and stable humidity control [49]. The experimental results of the dehumidification process are illustrated in Figure 14.

The blue line indicates the external relative humidity (78–85% RH), while the orange line shows the internal humidity controlled by alternating Silica Gel A and B. Both gels demonstrate similar moisture absorption performance, reducing indoor humidity to as low as 45% RH and averaging 54.37% RH per cycle. Each cycle lasts approximately 1 hour and 30 minutes. While one silica gel unit operates, the other undergoes heat-based regeneration. This alternating process ensures continuous and stable humidity control within the isolation room.

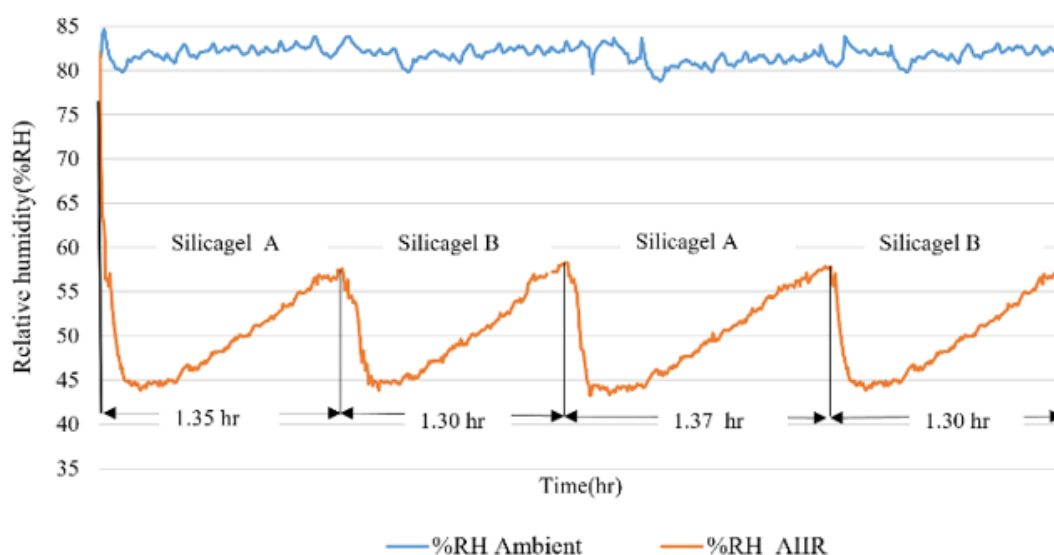
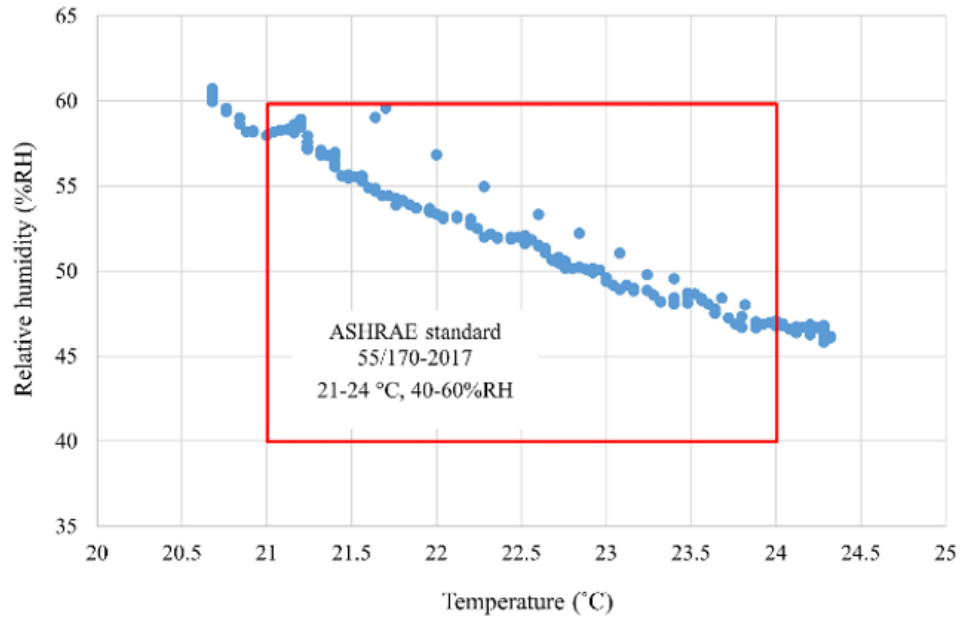
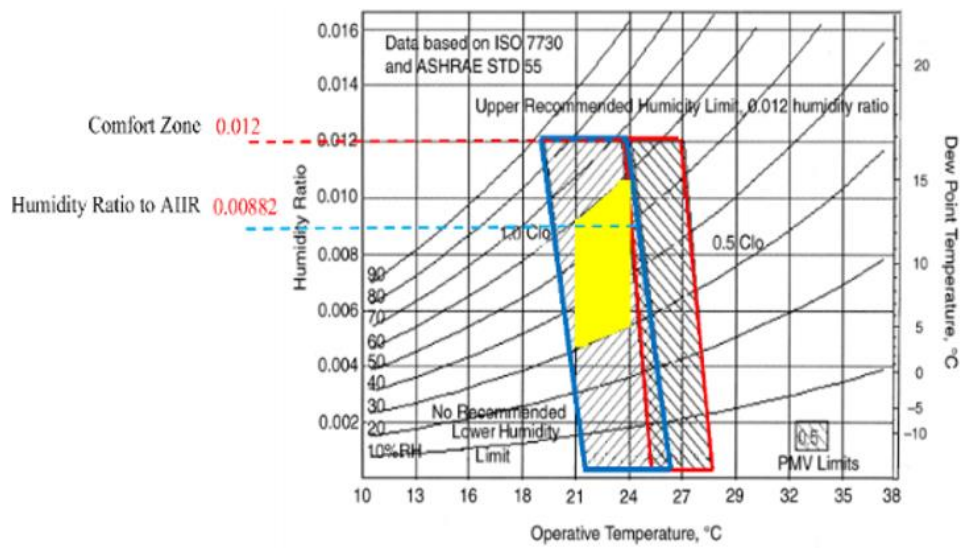


Figure 14. Dehumidification performance using Silica gel A and B





**Figure 15.** Distribution of relative humidity and temperature in AIIRs



**Figure 16.** Comparison of humidity ratio in airborne infection isolation rooms with standard values

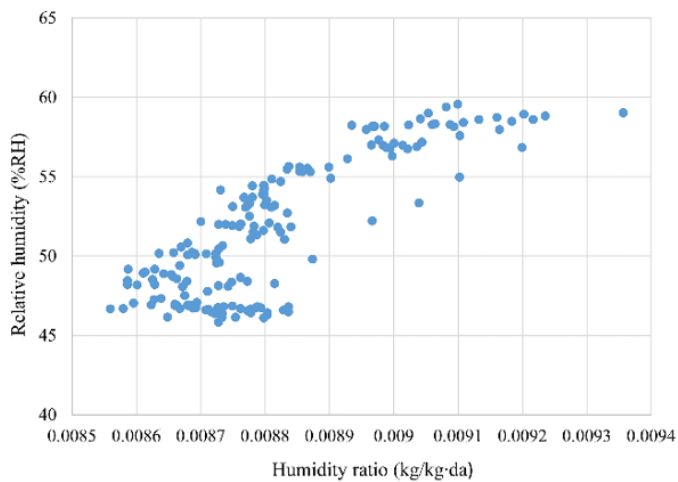


**Figure 17.** Evaluation of humidity control performance based on RH and humidity ratio

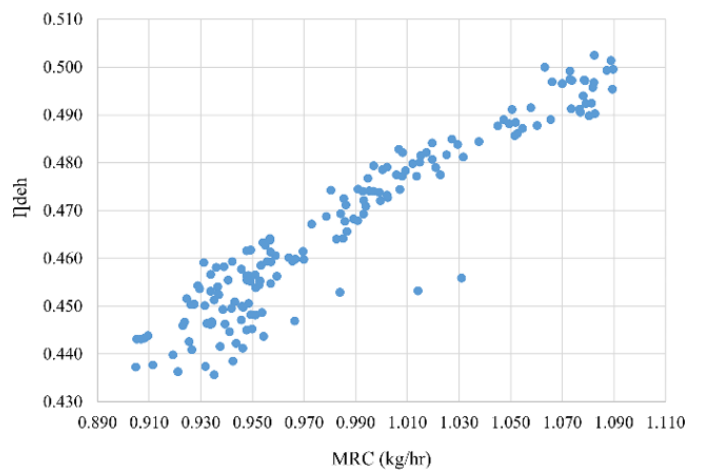


**Figure 18.** Relationship between adsorption efficiency and moisture removal capacity of the humidity control system

Figure 15 illustrates that most temperature and humidity data points in the isolation room remained within the desired range, confirming that the system is effective in maintaining stable conditions. While some deviations occurred due to external factors, the average temperature and relative humidity were 22.63°C and 54.37% RH, respectively indicating consistent environmental control.

Figure 16 illustrates the comfort zone for temperature and humidity ratio in AIIRs. The yellow box marks the acceptable range, with the red dashed line at the maximum limit of 0.012 kg/kg·da. The measured value, shown by the blue dashed line, is 0.00882 kg/kg·da within standard limits. This confirms effective humidity control, supporting infection prevention and patient safety.

#### 4.2 Performance evaluation based on relative humidity and humidity ratio

The relationship between relative humidity (RH) and humidity ratio (HR) is critical for ensuring accurate and energy efficient humidity control in AIIRs. RH, being temperature-dependent, may fluctuate with ambient temperature changes and potentially result in misinterpretation when used as a sole parameter. For instance, a decrease in temperature may cause an increase in RH without any actual rise in moisture content, leading to unnecessary dehumidifier activation. In contrast, HR is an absolute indicator of moisture content in the air and remains stable regardless of temperature variations, providing more reliable input for automated control systems. Maintaining RH below 60% is also vital, as higher RH levels promote microbial growth in HVAC systems, thereby increasing the risk of infection. Monitoring both RH and HR enables environmental control systems to maintain more stable indoor air quality, prevent false system responses, and enhance patient safety particularly in tropical climates where temperature fluctuations are frequent [50, 51].

The scatter plot presented in Figure 17 illustrates a positive correlation between humidity ratio (0.0084–0.0094 kg/kg·da) and relative humidity (40–60% RH) within the AIIR. As the humidity ratio increases, the relative humidity correspondingly rises, indicating the effective performance of the humidity control system. While the majority of data points align with the expected trend, several outliers are observed when the humidity ratio exceeds 0.0092 kg/kg·da, suggesting

minor deviations under elevated moisture conditions.

#### 4.3 Adsorption efficiency and moisture removal performance

Moisture Removal Capacity (MRC) represents the amount of moisture a system can extract per hour, whereas adsorption efficiency indicates the system's ability to absorb and retain water vapor effectively. Both metrics are critical for evaluating the performance of humidity control systems, particularly in environments requiring precise regulation.

Figure 18 shows a strong positive correlation between MRC and adsorption efficiency. As MRC increases, so does efficiency, with data points forming a consistent linear trend, indicating stable and reliable system performance.

#### 4.4 Regeneration process for silica gel desiccant in AIIRs

The regeneration process is essential for maintaining silica gel’s moisture adsorption efficiency. In this experiment, heat was applied to release retained moisture through thermal diffusion. Controlled heating ensured safe desorption without damaging the gel. The results of this process are summarized below, as shown in Figure 19.

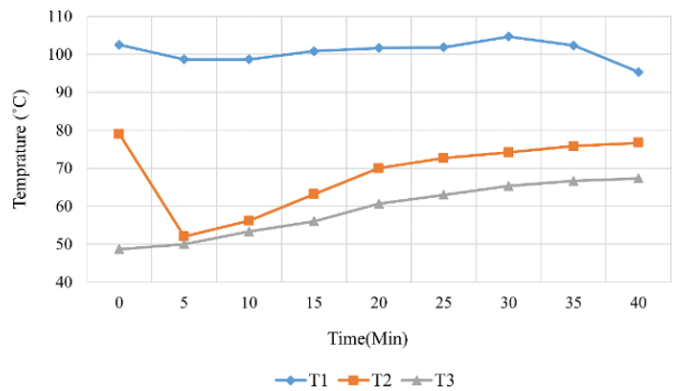


**Figure 19.** Temperature variation during the regeneration process  
T1: Air inlet temperature  
T2: Air outlet temperature  
T3: Air exhaust temperature

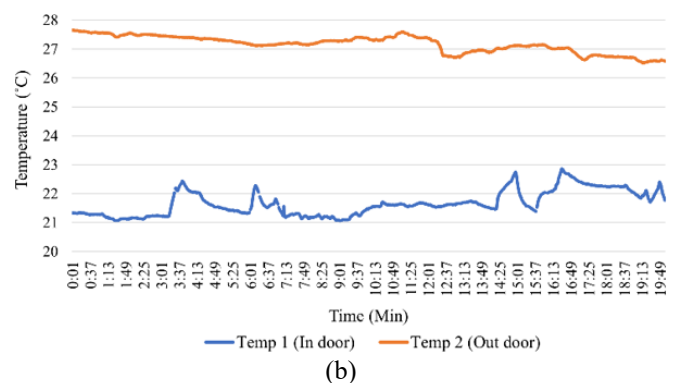
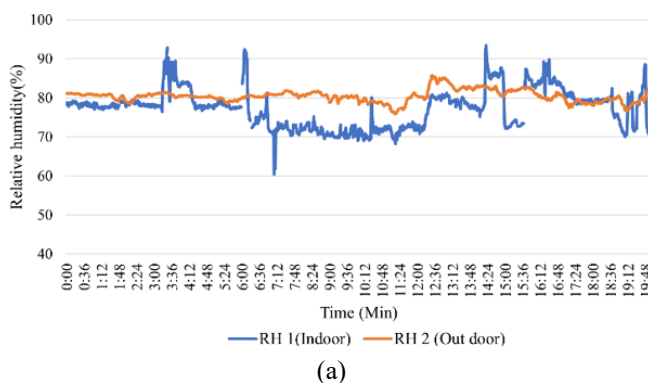


**Figure 20.** Data collection and analysis using Google Sheets

The moisture desorption process of silica gel begins at maximum moisture content, visually indicated by a pink coloration. Upon heating to 100°C (T1), moisture is rapidly released, followed by a gradual decline in desorption rate as

the gel approaches dryness. When fully regenerated, the silica gel turns blue, with the entire process taking approximately 55 minutes. The rear surface of the panel (T2) maintains an average temperature of 69°C, while the exhaust air

temperature (T3) averages 59°C, reflecting the system's internal heat transfer dynamics during regeneration.

#### 4.5 Monitoring and notification system

This system provides real-time temperature, and relative humidity data. The information is displayed at the room entrance, accompanied by audible alarms and flashing lights for notifications. Additionally, the data is accessible in real-time on smartphones, enhancing the convenience of monitoring.

Figure 20 illustrates effective real-time monitoring using Google Sheets. Graph (a) shows stable indoor temperature compared to outdoor fluctuations, while Graph (b) shows controlled indoor humidity. The system alerts users when values exceed limits, enabling timely intervention.

Table 3 shows real-time monitoring of temperature, humidity, and pressure from the environmental sensor system. The data includes timestamped entries collected via the BME280 sensor and transmitted through the IoT-based monitoring platform.

**Table 3.** Data logging using Google Sheets

Number Sensor	Date	Time	Temperature	Humidity	Pressure
2	12/9/2022	0:02:03	23.93	83.25	100,982.92
1	12/9/2022	0:01:01	27	75.3	100,929.81
2	12/9/2022	0:03:01	23.93	83.24	100,982.92
1	12/9/2022	0:02:01	27.03	75.2	100,928.39
1	12/9/2022	0:03:00	27.04	75.15	100,925.84
2	12/9/2022	0:04:00	23.94	83.19	100,978.04
2	12/9/2022	0:05:03	23.95	83.19	100,976.66
2	12/9/2022	0:06:01	23.96	83.08	100,976.70
1	12/9/2022	0:05:01	27.07	75.04	100,923.98
2	12/9/2022	0:07:01	23.97	83.09	100,976.75
1	12/9/2022	0:06:02	27.10	74.98	100,920.98
1	12/9/2022	0:07:01	27.11	74.95	100,916.71
2	12/9/2022	0:08:04	23.97	83.12	100,974.03
1	12/9/2022	0:06:54	27.11	74.84	100,917.19
1	12/9/2022	0:07:04	27.12	74.79	100,919.63
2	12/9/2022	0:09:02	23.98	83.08	100,970.00
1	12/9/2022	0:08:08	27.13	74.83	100,916.80
1	12/9/2022	0:09:05	27.14	74.77	100,916.01
1	12/9/2022	0:10:01	27.15	74.78	100,912.83
2	12/9/2022	0:11:05	23.98	83.03	100,967.29
1	12/9/2022	0:11:00	27.15	74.66	100,910.64
2	12/9/2022	0:12:05	23.98	83	100,969.16
2	12/9/2022	0:13:03	23.97	83.01	100,968.94

## 5. CONCLUSION

These conclusions underscore the stability of temperature and relative humidity within AIIRs, as well as the effectiveness of the environmental control system in maintaining conditions that comply with recommended standards. The study was conducted through a comprehensive process of measurement and performance evaluation of an IoT-integrated system, which enabled real-time monitoring and analysis. The key findings are summarized as follows:

- **Stability of temperature and humidity**

The control of temperature within the AIIRs at 22.63°C and relative humidity at 54.37% RH complies with ASHRAE Standard 55/170-2017 and ISO 7730. These values indicate thermal comfort and effective room temperature and humidity regulation. The ability of the system to maintain this stability significantly reduces the risk of airborne infection transmission.

- **Relationship between humidity ratio and relative humidity**

The system demonstrates a positive correlation between the humidity ratio and relative humidity within the AIIRs. This relationship reflects the responsiveness of the system to changes in humidity levels and highlights its effectiveness in managing and maintaining the desired humidity conditions.

- **Monitoring and notifications**

The system provides real-time monitoring through Google Sheets and Apps Script, enabling remote access and management of environmental conditions. Automated alerts via smartphone notifications and on-site alarms ensure timely corrective actions, enhancing operational efficiency and environmental control in AIIRs.

## ACKNOWLEDGMENT

The authors sincerely thank Betong Hospital for its support and collaboration throughout this research. The assistance provided by the hospital staff, along with the resources and data collection support, was essential to the success of this study. The dedication and cooperation of all individuals involved significantly contributed to achieving the research goals.

## REFERENCES

- [1] World Health Organization (WHO). (2020). Report of the WHO-China joint mission on coronavirus disease 2019 (COVID-19). Geneva: World Health Organization.

- [2] Wang, C.C., Prather, K.A., Sznitman, J., Jimenez, J.L., Lakdawala, S.S., Tufekci, Z., Marr, L.C. (2021). Airborne transmission of respiratory viruses. *Science*, 373(6558): eabd9149. <https://doi.org/10.1126/science.abd9149>
- [3] Qiu, G.Y., Zhang, X.L., deMello, A.J., Yao, M.S., Cao, J.J., Wang, J. (2023). On-site airborne pathogen detection for infection risk mitigation. *Chemical Society Reviews*, 52(24): 8531-8579. <https://doi.org/10.1039/D3CS00417A>
- [4] Argyropoulos, C.D., Skoulou, V., Efthimiou, G., Michopoulos, A.K. (2023). Airborne transmission of biological agents within the indoor built environment: A multidisciplinary review. *Air Quality, Atmosphere & Health*, 16(3): 477-533. <https://doi.org/10.1007/s11869-022-01286-w>
- [5] Di Gennaro, F., Petrosillo, N. (2022). New endemic and pandemic pathologies with interhuman airborne transmission through ear, nose and throat anatomical sites. *Acta Otorhinolaryngologica Italica*, 42(Suppl 1): S5. <https://doi.org/10.14639/0392-100X-suppl.1-42-2022-01>
- [6] Tang, H.J., Lai, C.C., Chao, C.M. (2022). The collateral effect of COVID-19 on the epidemiology of airborne/droplet-transmitted notifiable infectious diseases in Taiwan. *Antibiotics*, 11(4): 478. <https://doi.org/10.3390/antibiotics11040478>
- [7] Fadem, S.Z. (2021). The airborne dilemma. *Arch Clin Nephrol*, 7(1): 006-008. <https://doi.org/10.17352/acn.000050>
- [8] Wu, Y., Jing, W.Z., Liu, J., Ma, Q.Y., Yuan, J., Wang, Y.P., Du, M., Liu, M. (2020). Effects of temperature and humidity on the daily new cases and new deaths of COVID-19 in 166 countries. *Science of the Total Environment*, 729: 139051. <https://doi.org/10.1016/j.scitotenv.2020.139051>
- [9] Pöhlker, M.L., Pöhlker, C., Krüger, O.O., Förster, J.D., et al. (2023). Respiratory aerosols and droplets in the transmission of infectious diseases. *Reviews of Modern Physics*, 95(4): 045001. <https://doi.org/10.1103/RevModPhys.95.045001>
- [10] Vijaykrishna, G., Balaji, G. (2023). Impact of indoor temperature and humidity in IAQ of health care buildings. *Civil Engineering and Architecture*, 11(3): 1273-1279.
- [11] American Society of Heating, Refrigerating and Air-Conditioning Engineers (ASHRAE). (2017). ASHRAE Standard 170 Handbook. ASHRAE, Atlanta, Georgia, USA. <https://www.ashrae.org/technical-resources/standards-and-guidelines/standards-addenda/ansi-ashrae-ashe-standard-170-2017-ventilation-of-health-care-facilities>.
- [12] Healthcare Infection Control Practices Advisory Committee (HICPAC). (2019). Guidelines for environmental infection control in health-care facilities. U.S. Department of Health and Human Services, Centers for Disease Control and Prevention (CDC), Atlanta, Georgia, USA. <https://www.cdc.gov/infection-control/media/pdfs/guideline-environmental-h.pdf>
- [13] Qian, H., Li, Y.G., Seto, W.H., Ching, P., Ching, W.H., Sun, H.Q. (2010). Natural ventilation for reducing airborne infection in hospitals. *Building and Environment*, 45(3): 559-565. <https://doi.org/10.1016/j.buildenv.2009.07.011>
- [14] Tang, J.W., Li, Y., Eames, I., Chan, P.K.S., Ridgway, G.L. (2006). Factors involved in the aerosol transmission of infection and control of ventilation in healthcare premises. *Journal of Hospital Infection*, 64(2): 100-114. <https://doi.org/10.1016/j.jhin.2006.05.022>
- [15] Kohanski, M.A., Lo, L.J., Waring, M.S. (2020). Review of indoor aerosol generation, transport, and control in the context of COVID-19. *International Forum of Allergy & Rhinology*, 10(10): 1173-1179. <https://doi.org/10.1002/alar.22661>
- [16] Chen, W.Z., Zhang, N., Wei, J.J., Yen, H.L., Li, Y. (2020). Short-range airborne route dominates exposure of respiratory infection during close contact. *Building and Environment*, 176: 106859. <https://doi.org/10.1016/j.buildenv.2020.106859>
- [17] Lowen, A.C., Mubareka, S., Steel, J., Palese, P. (2007). Influenza virus transmission is dependent on relative humidity and temperature. *PLoS Pathogens*, 3(10): e151. <https://doi.org/10.1371/journal.ppat.0030151>
- [18] Yang, W., Marr, L.C. (2012). Mechanisms by which ambient humidity may affect viruses in aerosols. *Applied and Environmental Microbiology*, 78(19): 6781-6788. <https://doi.org/10.1128/AEM.01658-12>
- [19] Noti, J.D., Blachere, F.M., McMillen, C.M., Lindsley, W.G., Kashon, M.L., Slaughter, D.R., Beezhold, D.H. (2013). High humidity leads to loss of infectious influenza virus from simulated coughs. *PloS One*, 8(2): e57485. <https://doi.org/10.1371/journal.pone.0057485>
- [20] Morawska, L., Cao, J. (2020). Airborne transmission of SARS-CoV-2: The world should face the reality. *Environment International*, 139: 105730. <https://doi.org/10.1016/j.envint.2020.105730>
- [21] Tellier, R., Li, Y., Cowling, B.J., Tang, J.W. (2019). Recognition of aerosol transmission of infectious agents: A commentary. *BMC Infectious Diseases*, 19(1): 101. <https://doi.org/10.1186/s12879-019-3707-y>
- [22] ASHRAE. (2020). ASHRAE position document on infectious aerosols. ASHRAE, Atlanta, GA, USA. [https://www.ashrae.org/file%20library/about/position%20documents/pd\\_infectiousaerosols\\_2020.pdf](https://www.ashrae.org/file%20library/about/position%20documents/pd_infectiousaerosols_2020.pdf).
- [23] Arundel, A.V., Sterling, E.M., Biggin, J.H., Sterling, T.D. (1986). Indirect health effects of relative humidity in indoor environments. *Environmental Health Perspectives*, 65: 351-361. <https://doi.org/10.1289/ehp.8665351>
- [24] Sookchaiya, T., Monyakul, V., Thepa, S. (2010). Assessment of the thermal environment effects on human comfort and health for the development of novel air conditioning system in tropical regions. *Energy and Buildings*, 42(10): 1692-1702. <https://doi.org/10.1016/j.enbuild.2010.04.012>
- [25] Matung, T., Sookchaiya, T., Nangtin, P. (2021). Assessment of the indoor air quality and energy consumption of the AIIR Betong hospital. In 2021 18th International Conference on Electrical Engineering/Electronics, Computer, Telecommunications and Information Technology (ECTI-CON), Chiang Mai, Thailand, pp. 733-736. <https://doi.org/10.1109/ECTI-CON51831.2021.9454899>
- [26] Hamdani, H., Sabri, F.S., Harapan, H., Syukri, M., Razali, R., Kurniawan, R., Irwansyah, I., Sofyan, S.E., Mahlia, T.M.I., Rizal, S. (2022). HVAC control systems for a negative air pressure isolation room and its performance. *Sustainability*, 14(18): 11537.



- <https://doi.org/10.3390/su141811537>
- [27] Mehare, H.B., Hussain, T., Zia, M.A., Saleem, S. (2025). Performance evaluation of a rotary dehumidifier with molecular sieve desiccant using coupled regeneration mode: Experimental investigation. *Energy and Built Environment*, 6(2): 219-229. <https://doi.org/10.1016/j.enbenv.2023.10.008>
  - [28] Wang, C., Zhang, X., Li, Y. (2021). Airflow management in negative pressure isolation rooms: Effect of diffuser placement and ventilation layout. *Building and Environment*, 197: 107866. <https://doi.org/10.1016/j.buildenv.2021.107866>
  - [29] Nie, J., Zhou, J., Li, G. (2021). Comparison of solid desiccants for air dehumidification: MIL-101(Cr) versus conventional materials. *Applied Thermal Engineering*, 198: 117499. <https://doi.org/10.1016/j.applthermaleng.2021.117499>
  - [30] Urrutia, A.R., Schlener, S.D., Eid, S., Bock, K.A., Worrlow, K.C. (2023). The effects of an advanced air purification technology on environmental and clinical outcomes in a long-term care facility. *The Journals of Gerontology: Series A*, 78(12): 2325-2332. <https://doi.org/10.1093/gerona/glad113>
  - [31] Stevenson, A., Freeman, J., Jermy, M., Chen, J. (2023). Airborne transmission: A new paradigm with major implications for infection control and public health. *The New Zealand Medical Journal (Online)*, 136(1570): 69-77.
  - [32] Thornton, G.M., Fleck, B.A., Dandnayak, D., Kroeker, E., Zhong, L., Hartling, L. (2022). The impact of heating, ventilation and air conditioning (HVAC) design features on the transmission of viruses, including the 2019 novel coronavirus (COVID-19): A systematic review of humidity. *PLoS One*, 17(10): e0275654. <https://doi.org/10.1371/journal.pone.0275654>
  - [33] Bahramnia, P., Hosseini Rostami, S.M., Wang, J., Kim, G.J. (2019). Modeling and controlling of temperature and humidity in building heating, ventilating, and air conditioning system using model predictive control. *Energies*, 12(24): 4805. <https://doi.org/10.3390/en12244805>
  - [34] Thiyaneswaran, B., Anguraj, K., Kumarganesh, S., Ghosh, S. (2022). IOT based smart cold chain temperature monitoring and alert system for vaccination container. *Przeglad Elektrotechniczny*, 98(8): 206-208. <https://doi.org/10.15199/48.2022.08.38>
  - [35] Ali, Y., Khan, H.U. (2023). IoT platforms assessment methodology for COVID-19 vaccine logistics and transportation: A multi-methods decision making model. *Scientific Reports*, 13(1): 17575. <https://doi.org/10.1038/s41598-023-44966-y>
  - [36] Jiang, S.J., Jia, S.M., Guo, H.J. (2024). Internet of Things (IoT)-enabled framework for a sustainable vaccine cold chain management system. *Heliyon*, 10(7): e28910. <https://doi.org/10.1016/j.heliyon.2024.e28910>
  - [37] Hassan, A.A., Tutuncu, K., Abdullahi, H.O., Ali, A.F. (2023). IoT-based smart health monitoring system: Investigating the role of temperature, blood pressure and sleep data in chronic disease management. *Instrumentation Measure Métrologie*, 22(6): 231-240. <https://doi.org/10.18280/i2m.220602>
  - [38] Ghani, N.M.A., Lim, W.J., Hoh, W.S., Hassan, S.A.A. (2024). Rehabilitation and home health monitoring based-AI scheduling application for coronary artery disease and cardiovascular patients. *Instrumentation Measure Métrologie*, 23(2): 161-173. <https://doi.org/10.18280/i2m.230207>
  - [39] Rahita, A.C., Zaki, A., Nugroho, G., Yadi, S. (2024). Internet of Things (IoT) in structural health monitoring: A decade of research trends. *Instrumentation Measure Métrologie*, 23(2): 123-139. <https://doi.org/10.18280/i2m.230205>
  - [40] AbdelRaheem, M., Hassan, M., Mohammed, U.S., Nassr, A.A. (2022). Design and implementation of a synchronized IoT-based structural health monitoring system. *Internet of Things*, 20: 100639. <https://doi.org/10.1016/j.iot.2022.100639>
  - [41] Nasution, A.M.T., Ibrahim, I.A., Asani, P.A.A., Anggara, Y. (2022). Performance evaluation of the webcam-based contactless respiratory rate monitoring system. *Instrumentation Measure Métrologie*, 21(6): 217-223. <https://doi.org/10.18280/i2m.210602>
  - [42] Engineering Institute of Thailand (EIT). (2020). Manual for constructing and adapting negative pressure cabinets (Revision 3) [Technical manual]. <https://www.eit.or.th>
  - [43] Noui, S., Bougoul, S., Demagh, Y. (2021). Interaction between the turbulent natural convection and surface radiation inside a confined greenhouse. *International Journal of Heat and Technology*, 39(1): 51-60. <https://doi.org/10.18280/ijht.390106>
  - [44] Khoukhi, M., Al Khatib, O. (2021). Performance of desiccant-based cooling systems in hot-humid climates: A review. *Energy Engineering*, 118(4): 875-909. <https://doi.org/10.32604/ee.2021.015835>
  - [45] Wang, F., Chaerasari, C., Rakshit, D., Permana, I., Kusnandar, K. (2021). Performance improvement of a negative-pressurized isolation room for infection control. *Healthcare*, 9(8): 1081. <https://doi.org/10.3390/healthcare9081081>
  - [46] Halawa, E., Bruno, F. (2023). Energy performance and thermal comfort delivery capabilities of solid-desiccant rotor-based air conditioning for warm to hot and humid climates a critical review. *Energies*, 16(16): 6032. <https://doi.org/10.3390/en16166032>
  - [47] Ge, T.S., Qi, D., Dai, Y.J., Wang, R.Z. (2018). Experimental testing on contaminant and moisture removal performance of silica gel desiccant wheel. *Energy and Buildings*, 176: 71-77. <https://doi.org/10.1016/j.enbuild.2018.07.033>
  - [48] Kubota, M., Hanaoka, N., Matsuda, H., Kodama, A. (2017). Dehumidification behavior of cross-flow heat exchanger type adsorber coated with aluminophosphate zeolite for desiccant humidity control system. *Applied Thermal Engineering*, 122: 618-625. <https://doi.org/10.1016/j.applthermaleng.2017.05.047>
  - [49] Chua, H.T., Ng, K.C., Chakraborty, A., Oo, N.M., Othman, M.A. (2002). Adsorption characteristics of silica gel+ water systems. *Journal of Chemical & Engineering Data*, 47(5): 1177-1181. <https://doi.org/10.1021/je0255067>
  - [50] World Health Organization (WHO). (2021). Roadmap to improve and ensure good indoor ventilation in the context of COVID-19. WHO, Geneva, Switzerland. <https://iris.who.int/bitstream/handle/10665/339857/9789240021280-eng.pdf?sequence=1>
  - [51] Taal, A., Itard, L. (2020). P&ID-based automated fault identification for energy performance diagnosis in HVAC systems: 4S3F method, development of DBN

## Greek symbols

$\rho$	density of air ( $\text{kg}/\text{m}^3$ )
$\omega$	humidity ratio ( $\text{kg} / \text{kg}$ dry air)

## Subscripts

p	dehumidification
w	water vapour
da	dry air

## NOMENCLATURE

RH	Relative humidity
MRC	Moisture removal capacity ( $\text{Kg}/\text{h}$ )
$\eta_{deh}$	Dehumidification effectiveness
V	Velocity ( $\text{m}/\text{s}$ )
$\omega_1$	Inlet humidity ratio ( $\text{kg} / \text{kg}$ dry air)
$\omega_2$	Outlet humidity ratio ( $\text{kg} / \text{kg}$ dry air)